

Development of Austenitic Stainless Steel with Reduced Nickel and Molybdenum for Bipolar Plates of PEFCs

Kotaro SEKIMUKAI*
Toru MATSUHASHI

Kazunari IMAKAWA
Manabu OKU

Abstract

As a bipolar plate material that is a major component of polymer electrolyte fuel cells (PEFCs), austenitic stainless steel, which is cheaper and has a higher performance than conventional carbon, is attracting attention. Although SUS316L has been studied in many cases, this article examined suitable ingredients with better cost performance. The developed steel 218N, which reduces Ni and Mo by adding nitrogen, saves resources and is superior in price stability compared to SUS316L. 218N has better metal elution resistance than SUS316L and can be applied as a bipolar plate material.

1. Introduction

Fuel cells (FCs) are gaining attention as a clean energy source, as they generate electricity using hydrogen as fuel. Among the various types of fuel cells, polymer electrolyte fuel cells (PEFCs) stand out for their ability to operate at low temperatures ranging from 70 to 90°C while maintaining high output density. As a result, PEFCs are increasingly being utilized as batteries in automobiles and households.¹⁻³⁾

Figure 1 shows a schematic diagram of the PEFC,¹⁾ where a gas diffusion layer (GDL) and a membrane electrode assembly (MEA) are sandwiched between bipolar plates. The bipolar plate material needs formability as they form a gas flow path. The region between the bipolar plate and the MEA serves as an environment where sulfate ions (SO_4^{2-}) and fluoride ions (F^-) elute from the electrolyte membrane in the MEA into humidifying water or water produced during power generation,⁴⁾ with chloride ions (Cl^-) being mixed in the water as well.⁵⁾ Additionally, on the cathode side, the potential is theoretically 1.23 V (based on the standard hydrogen electrode (SHE)). In reality, it ranges from about 0.6 to 1.0 V. Consequently, there is a possibility that the potential of the cathode bipolar plate may also increase to about that level.¹⁾ Furthermore, the contact area between the bipolar plate and the GDL may become a fine gap structure. Crevice corrosion resistance is thus required in the environment mentioned above.⁶⁾

SUS316L, a widely used austenitic stainless steel, offers excellent corrosion resistance and formability. However, its high content of rare metals like Mo and Ni contributes to price fluctuations. Ad-

ressing this concern, this study developed 218N (21Cr-8.3Ni-0.15N), a novel low-Ni, Mo-saving austenitic stainless steel specifically designed for PEFC bipolar plates. This paper first outlines the development process of 218N, followed by a detailed analysis of its key properties. Finally, it presents evaluations of commercially produced 218N steel sheets and explores the potential of 218N beyond the PEFC applications.

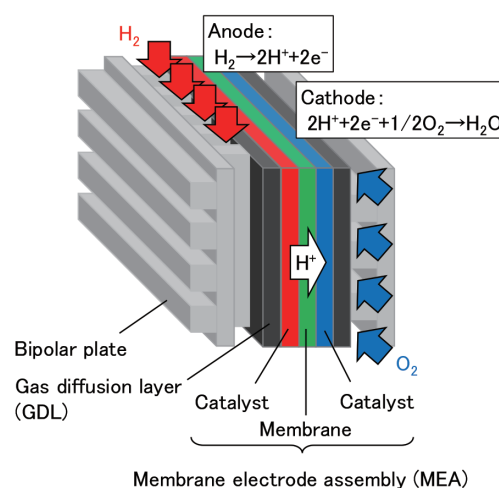


Fig. 1 Schematic image of PEFC

* Researcher, New Energy Material Research & Development Div., Research & Development Center, Nippon Steel Stainless Steel Corporation 3434 Ooaza-shimata, Hikari City, Yamaguchi Pref. 743-8550

2. Composition Design

Reducing the Mo content of SUS316L decreases the corrosion resistance, and excessively reducing the Ni content decreases the formability due to δ -ferrite phase precipitation. Therefore, in this study, we aimed to improve corrosion resistance by increasing the Cr content and to stabilize the γ phase by adding nitrogen (N). It is generally believed that the addition of Cr, Mo, and N is effective against the occurrence of local corrosion. But PEFC bipolar plates are in a special environment of high temperature, low pH, and high potential, so the effects of the respective elements may change. Therefore, we conducted a study focusing on the effects of Cr, Mo, and N in a simulated PEFC environment and found that the effects of Mo and N on corrosion resistance were small. Furthermore, an excessive addition of N makes the material hard and reduces its formability. Therefore, our development goals were: (1) to have crevice corrosion resistance equivalent to or better than SUS316L in the PEFC environment and (2) to have formability with a total extension at fracture (hereafter referred to as total extension) of 45% or more for fabrication into a bipolar plate shape.

3. Experimental

3.1 Test steel

Table 1 presents the chemical compositions of the test steel and control steels. The index used to gauge the stability of the γ phase was Md_{30} (Nohara's equation⁷⁾): $551-462(C+N)-9.2Si-8.1Mn-29.0(Ni+Cu)-13.7Cr-18.5Mo-68.0Nb$. Md_{30} represents the temperature (in °C) at which 50% of the microstructure transforms into martensite (α') when a true strain of 0.30 is applied to a single-phase γ sample. The test steel was produced through vacuum melting in a laboratory, followed by rolling, annealing, pickling, and forming into sheets with a thickness of 1.0 mm for crevice corrosion resistance evaluation. Additionally, cold rolling, annealing and pickling were performed on the sheets to reduce their thickness to 0.3 mm for formability evaluation purposes. The grain size numbers for all samples were approximately set at 7.

3.2 Crevice corrosion resistance

Figure 2 provides a schematic representation of a crevice corrosion test specimen. The specimen was obtained by cutting a sample sheet to a size of 30×30 mm and drilling a hole 6.5 mm in diameter at the center. The surfaces of the specimen were wet polished to #600. When assembling the test setup, the specimen was placed between resin gaskets and secured using titanium washers, a titanium bolt, and a titanium nut. A test solution was prepared by mixing special grade reagents NaF, NaCl, H₂SO₄, and pure water. The test solution was adjusted to 3 ppm F⁻+10 to 50 ppm Cl⁻, with a pH value of 3.0. The temperature of the solution was maintained at 90°C. The specimen was immersed in the prepared solution and subjected to a constant potential of 0.9 V for 6 h. This allowed for determining the minimum concentration of Cl⁻ required for localized corrosion to occur. The occurrence of local corrosion was assessed through external observation using an optical microscope.

3.3 Formability

Formability was assessed by a room temperature tensile test. No. 13B specimens, following the guidelines of JIS Z 2241, were obtained to ensure that the rolling direction aligned with the tensile direction. The total extension of the specimens was measured using the tensile test method specified in JIS Z 2241.

Table 1 Chemical compositions

| | (mass%) | | | | | | | | |
|------------|---------|-----|---------|-----------|---------|-----|----------|-----------|-------------------|
| | C | Si | Mn | Cr | Ni | Mo | Cu | N | Md_{30} (°C) |
| Test steel | 0.07 | 0.4 | 0.8–3.0 | 21.0–23.0 | 7.0–9.0 | – | 0.20–3.0 | 0.10–0.19 | –57– –115 |
| SUS316L | 0.02 | 0.5 | 1.7 | 17.3 | 12.1 | 2.1 | 0.4 | 0.01 | –120 |
| SUS304 | 0.07 | 0.5 | 0.8 | 18.4 | 8.1 | – | 0.3 | 0.02 | 4 |
| SUS310S | 0.01 | 0.6 | 0.4 | 25.6 | 19.3 | – | 0.2 | 0.03 | –394 |
| SUS315J2 | 0.04 | 2.8 | 0.5 | 18.3 | 12.0 | 0.8 | 2.0 | 0.01 | –173 |
| SUS304N1 | 0.08 | 0.7 | 1.8 | 18.3 | 10.2 | – | – | 0.14 | –117 |

$$Md_{30} = 551 - 462(C + N) - 9.2Si - 8.1Mn - 29.0(Ni + Cu) - 13.7Cr - 18.5Mo - 68.0Nb$$

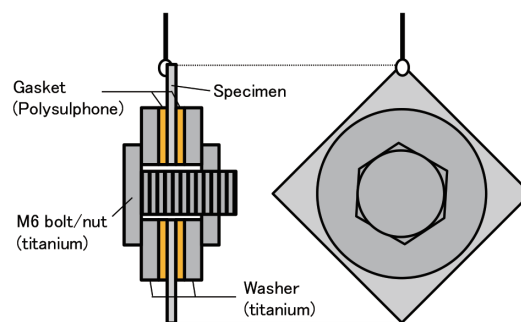


Fig. 2 Schematic image of crevice corrosion test specimen

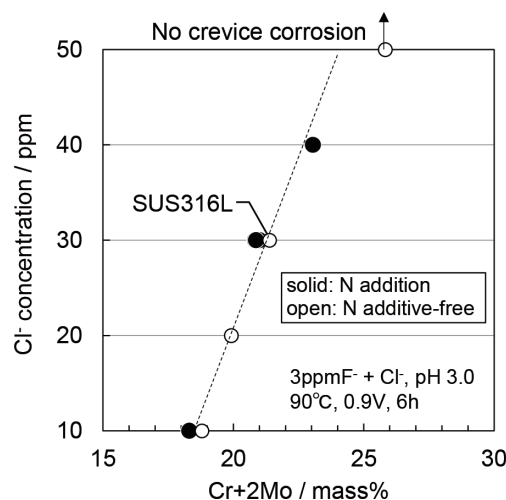


Fig. 3 Relationship between alloying elements and Cl⁻ concentration at which crevice corrosion occurred

4. Results and Discussion

4.1 Crevice corrosion resistance

Figure 3 illustrates the results obtained from the evaluation of crevice corrosion resistance. The Cl⁻ concentration at which crevice corrosion occurred in the simulated PEFC environment can be summarized using the [Cr+2Mo] value, irrespective of the presence of N. For SUS316L with a [Cr+2Mo] value of 21.4, crevice corrosion was observed at a Cl⁻ concentration of 30 ppm or higher. No crevice corrosion was observed at Cl⁻ concentrations below 20 ppm. Interestingly, even with the test steel 218N that did not contain Mo but had

a [Cr+2Mo] value of 21.0 and was alloyed with 21% Cr, no crevice corrosion occurred at Cl⁻ concentrations of 20 ppm or lower. This suggests that the crevice corrosion resistance exhibited by 218N is comparable to or better than that of SUS316L. Cr, Mo, and N are generally considered to be effective in suppressing the occurrence of crevice corrosion. The effects of Cr, Mo, and N in the simulated PEFC environment are discussed below.

Cr is the primary element that forms the passive film on stainless steel. Generally, a higher Cr content in steels leads to improved resistance against crevice corrosion. Increasing the Cr content is also effective in the simulated PEFC environment and is believed to contribute to enhancing crevice corrosion resistance. Referring to the potential-pH diagram for the Cr-H₂O system,⁸⁾ it can be observed that at pH 3.0 and 0.9 V, Cr remains stable in the HCrO₄⁻ state. Although transpassive dissolution may occur, its rate is significantly low. It is presumed that the passive film acts as a corrosion resistant film while undergoing transpassive dissolution.

Mo is known as an element that significantly improves crevice corrosion resistance. In general, steels with a higher Mo content have better crevice corrosion resistance. Increasing the Mo content was effective even in the simulated PEFC environment and is thought to have contributed to improving crevice corrosion resistance. According to the potential-pH diagram for the Mo-H₂O system,⁹⁾ at pH 3.0 and 0.9 V, Mo is stable in the MoO₄²⁻ state, and it is thought that transpassive dissolution is occurring. Furthermore, the equilibrium potential of the transpassive dissolution reaction of Mo (e.g., MoO₂/MoO₄²⁻) is said to be on the much less noble side than that of Cr.¹⁰⁾ At a noble potential of 0.9 V, its contribution to corrosion resistance is considered to become small.

N is generally recognized as an element that can enhance crevice corrosion resistance. However, no clear effect of N was observed in the simulated PEFC environment. Referring to the potential-pH diagram for the NH₃-H₂O system,¹¹⁾ it is evident that at pH 3.0 and 0.9 V, N remains stable in the NO₃⁻ state. It is believed that N acts as an inhibitor, suppressing the attack of Cl⁻ on the passive film.¹²⁾ However, when crevice corrosion occurs, there is a significant decrease in pH inside the crevice. This condition suggests that NH₄⁺ becomes stable. The inhibitory effect of NH₄⁺ on corrosion has been reported to diminish in high-temperature aqueous solutions.¹³⁾ Many aspects regarding the impact of N in the simulated PEFC environment remain unknown, and further investigation is necessary in this regard.

Based on the previous discussion, it is evident that in order for 218N to exhibit crevice corrosion resistance equivalent to or better than that of SUS316L in the simulated PEFC environment, the [Cr+2Mo] value needs to be 21 or higher. Considering the compositional design concept aimed at reducing Mo usage, the steel 218N was developed with a composition of 21Cr-Ni-N (without adding Mo).

4.2 Formability

Figure 4 illustrates the effect of the Md₃₀ value and N content on the total extension at room temperature (25°C). All test specimens successfully met the desired target of achieving a total extension of 45% or higher. It was observed that when the N content ranged from 0.10% to 0.19%, a higher Md₃₀ value corresponded to a higher total extension. This can be attributed to an increased α' transformation during the tensile process, thereby improving ductility.¹⁴⁾ Furthermore, as the N content increased, the total extension tended to decrease. To consistently achieve a total extension of 45% or more, it is advisable to limit the N content to 0.19% or less. Additionally, if a

lower N content of 0.10% is desired to suppress the δ-ferrite phase precipitation, it would be necessary to increase the Ni content to at least 9.0%. However, this approach may result in diminishing the cost benefit associated with the reduction of the Ni content.

Based on the above discussion, the N content was set at 0.15% from the viewpoint of formability, and 21Cr-Ni-0.15N was selected as the basic composition of the developed steel 218N, taking into account the aforementioned examination of crevice corrosion resistance. Furthermore, from the perspective of suppressing the precipitation of the δ-ferrite phase, we commercially produced the 21Cr-8.3Ni-0.15N steel (the steel 218N) with a Ni content of 8.3%.

5. Properties of 218N

5.1 Representative compositions and mechanical properties

The chemical compositions of the 218N steel (21Cr-8.3Ni-0.15N) and control steels melted in an actual furnace are presented in Table 2. All specimens were cold rolled and annealed sheets with a thickness of 1.0 mm, and the grain size numbers were adjusted to about 8. Table 3 displays the mechanical properties of the specimens. While 218N exhibits a lower total extension compared to SUS316L and SUS304, it demonstrates higher values for the 0.2%

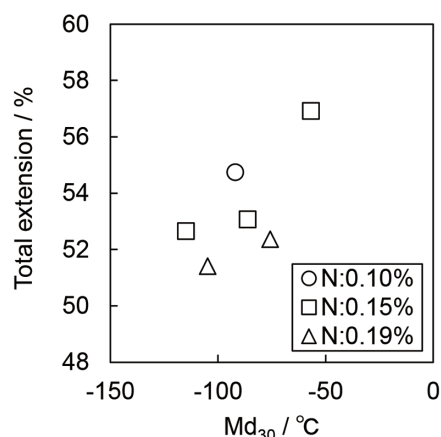


Fig. 4 Effect of Md₃₀ value and N contents on total extension value

Table 2 Chemical compositions

| | (mass%) | | | | | | | | |
|---------|---------|-----|-----|------|------|-----|-----|------|-----------------------|
| | C | Si | Mn | Cr | Ni | Mo | Cu | N | Md ₃₀ (°C) |
| 218N | 0.07 | 0.4 | 0.8 | 21.1 | 8.4 | — | 0.2 | 0.16 | -104 |
| SUS316L | 0.01 | 0.5 | 0.8 | 17.4 | 12.0 | 2.0 | 0.2 | 0.01 | -99 |
| SUS304 | 0.07 | 0.5 | 1.2 | 18.4 | 8.2 | — | 0.3 | 0.04 | -17 |

$$Md_{30} = 551 - 462(C+N) - 9.2Si - 8.1Mn - 29.0(Ni+Cu) - 13.7Cr - 18.5Mo - 68.0Nb$$

Table 3 Mechanical properties

| | 0.2%PS (MPa) | TS (MPa) | Total extension (%) | Hardness (HV) | Erichsen value (mm) |
|---------|--------------|----------|---------------------|---------------|---------------------|
| 218N | 395 | 725 | 49 | 179 | 12.1 |
| SUS316L | 276 | 565 | 52 | 136 | 13.5 |
| SUS304 | 304 | 646 | 54 | 166 | 13.4 |

proof stress (PS) and tensile strength (TS). If 218N can be formed into desired forms, such as PEFC bipolar plates, the higher the strength, the thinner the steel can be, potentially leading to reduced structural weight.

5.2 Crevice corrosion resistance and metal elution resistance

As stated earlier, 218N needs to exhibit crevice corrosion resistance comparable to SUS316L in the simulated PEFC environment. However, if crevice corrosion does not occur, there is still a concern regarding metal elution resulting from transpassive dissolution. It is reported that fluoride ions (F⁻) can enhance the transpassive dissolution process.¹⁵ In this section, 218N and SUS316L were compared in terms of their corrosion resistance in the simulated PEFC environment, specifically focusing on crevice corrosion resistance and metal elution resistance.

5.2.1 Crevice corrosion resistance

The crevice corrosion resistance of 218N was assessed under the same conditions as discussed in Section 3.2, and the results are presented in **Figure 5**. Similar to SUS316L, 218N does not exhibit crevice corrosion at Cl⁻ concentrations of 20 ppm or below, indicating its excellent resistance to this form of corrosion.

5.2.2 Metal elution resistance

The metal elution resistance of 218N was evaluated through potentiodynamic polarization and metal elution tests. Specimens measuring 15×20 mm were cut from the test steel and wet polished to #600 on the surfaces. Insulation silicone was applied to cover the specimen, leaving a 10×10 mm electrode surface for the potentiodynamic polarization test. A test solution with a pH of 3.0 and fluoride ion concentrations ranging from 0 to 100 ppm was prepared using high-grade reagents NaF, H₂SO₄, and pure water. The test solution was degassed with Ar and maintained at a temperature of 80°C. Each specimen was immersed in the test solution, and its potentiodynamic anodic polarization curve was measured at a sweep rate of 20 mV/min starting from the open-circuit potential. For the metal elution test, specimens measuring 30×30 mm were cut from the test steel and wet polished to #600 on the surfaces. The same test solution as that used in the potentiodynamic polarization test was utilized. The specimens were potentiostatically tested at a potential of 0.9 V for 72 h. The amount of metals eluted from each specimen

was determined using inductively coupled plasma mass spectrometry (ICP-MS).

Figure 6 shows the effect of F⁻ on the anodic polarization curves of the 218N specimens in a sulfuric acid solution with an F⁻ concentration of 0 to 100 ppm and a pH of 3.0. Up to about 0.8 V, the current density was about a few microamperes per centimeters squared (μA/cm²) regardless of the amount of F⁻, suggesting the presence of a good passive film. At 0 ppm of F⁻, a voltage region of 0.8 to 1.3 V was a transition region from the passive state to the transpassive state. The current density rose at a potential higher than 0.8 V but then dropped again due to the formation of a passive film of Fe. At 10 to 100 ppm of F⁻, the current density similarly rose at a potential higher than 0.8 V and increased as the F⁻ concentration increased. It is known that F⁻ destroys the passive film of Fe,^{15,16} probably because the addition of F⁻ promoted the dissolution of the base metal. Generally, the bipolar plates are expected to be used in the vicinity of 0.9 V, so it is thought that they must be protected from the transpassive dissolution of Cr, which causes the metal elution, and also protected from F⁻.

Figure 7 shows the amount of eluted metals after the potentiostatic polarization at 0.9 V for 72 h in the sulfuric acid solution to which F⁻ was added. The amount of eluted metals increased with the addition of F⁻ and was smaller for 218N than for SUS304 and

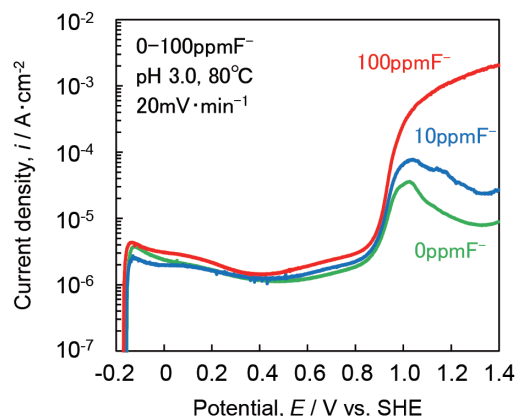


Fig. 6 Anode polarization curve of 218N in sulfuric acid solution to which 0–100 ppmF⁻ has been added

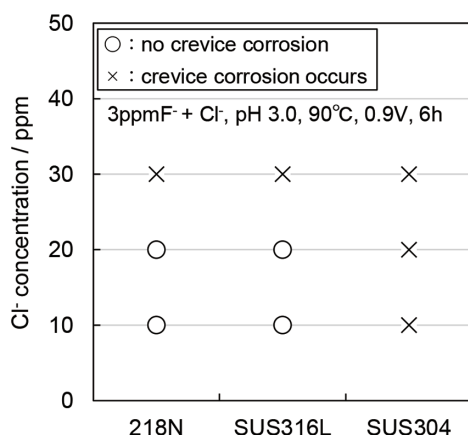


Fig. 5 Cl⁻ concentration of 218N and comparative material at which crevice corrosion occurred

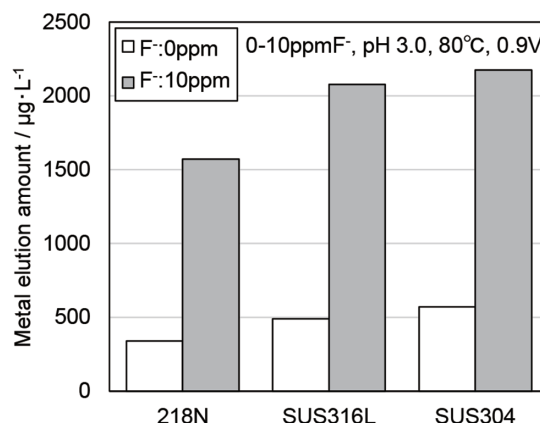


Fig. 7 Amount of metal elution after constant potential polarization in sulfuric acid solution to which F⁻ has been added at 0.9 V over 72 h

SUS316L. This means that 218N has superior metal elution resistance. It is reported that the higher the Cr content, the slower the corrosion rate up to a potential of about 1.3 V.¹⁷⁾ The steel 218N is considered to have excellent metal elution resistance for the same reason. Another possible reason is the elution of solute N as NO₃⁻ and the subsequent action of NO₃⁻ as an inhibitor to suppress the adsorption of F⁻ onto the steel surface.

5.3 Pitting corrosion resistance

Pitting corrosion resistance was evaluated by measuring the pitting potential. The solution was adjusted to 20000 ppm Cl⁻ using a NaCl reagent and was thoroughly degassed with Ar. The temperature was set at three levels of 30, 50, and 80°C, and the other conditions followed JIS G 0577. The specimens were dry polished to #600 on the surfaces immediately before the measurement. Potentiodynamic anodic polarization was performed from the open-circuit potential at a sweep rate of 20 mV/min, and the potential at which the current density reached 100 μA/cm² was defined as the pitting potential.

Figure 8 shows the effect of temperature on the pitting corrosion potential of three steels. All steels exhibited a relatively low pitting potential at a high temperature of 80°C. The pitting potential tended to increase as the temperature decreased. This tendency was particu-

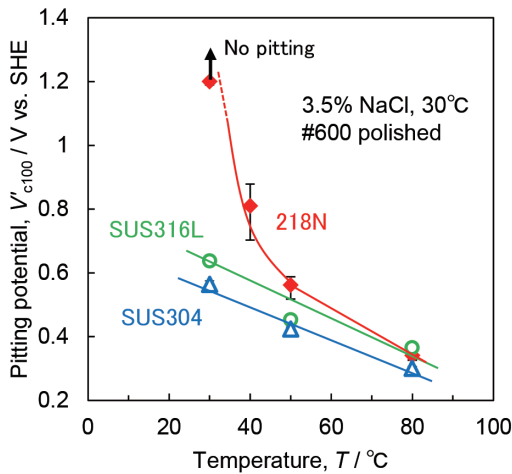


Fig. 8 Pitting potential at various temperatures

larly noticeable in the 218N steel alloyed with nitrogen. No pitting corrosion was observed in the solution at 30°C. This is probably because the pitting corrosion potential increased at low temperatures. Also, as mentioned above, nitrogen became stable in the NO₃⁻ state. Consequently, the pitting corrosion resistance markedly increased, and the pitting corrosion potential suddenly rose. These results suggested that 218N has pitting corrosion resistance exceeding that of SUS316L, especially near a room temperature of 30 to 50°C and under the effect of the nitrogen addition.

5.4 Atmospheric corrosion resistance

Atmospheric corrosion resistance was evaluated by an atmospheric exposure test on Miyakojima, Okinawa Prefecture. The specimens were wet polished to #400 on the surfaces. The atmospheric exposure test was conducted for one year at the Miyakojima exposure test site of the Japan Weathering Test Center (JWTC) in accordance with JIS Z 2381. The appearance of the specimens after the test was evaluated using the JIS G 0595 rating number (RN) on a scale of 10 from 0 to 9.

Figure 9 shows the appearance photographs of the specimens after one year of atmospheric exposure in Miyakojima. After the exposure to the atmosphere, the RN was 8 for 218N, 7 for SUS316L, and 4 for SUS304, and 218N showed weather resistance equal to or higher than that of SUS316L. Since the maximum temperature in Miyakojima during the exposure test was 34.6°C, this temperature range is believed to have enhanced the effect of the nitrogen addition to 218N, as described in Section 5.3. In other words, 218N is considered to have weather resistance equal to or higher than that of SUS316L, even in an atmospheric corrosion environment.

5.5 Magnetic properties

Low-magnetic austenitic stainless steels (SUS304, SUS316L, etc.) are often used for vacuum parts and electronic parts like portable game consoles to prevent the effects of magnetic fields and contaminant deposition. They are required to have high strength together with good magnetic properties. Cold-rolled and annealed steel sheets were again cold rolled to various rolling ratios. The relative magnetic permeability (average value of 5 specimens) and cross-sectional hardness (average value of 5 specimens at a load of 300 g) at each rolling ratio were measured. A List-Magnetik Ferromaster low-permeability meter was used to measure the relative magnetic permeability.

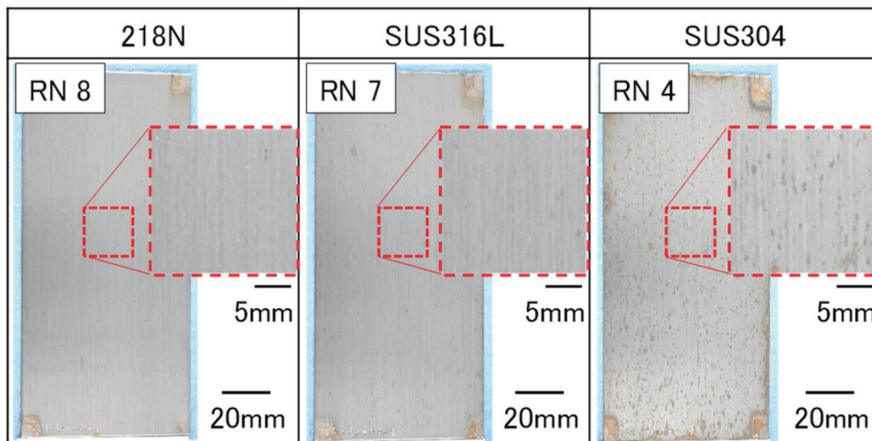


Fig. 9 Appearance of the specimens after 1 year of atmospheric exposure test

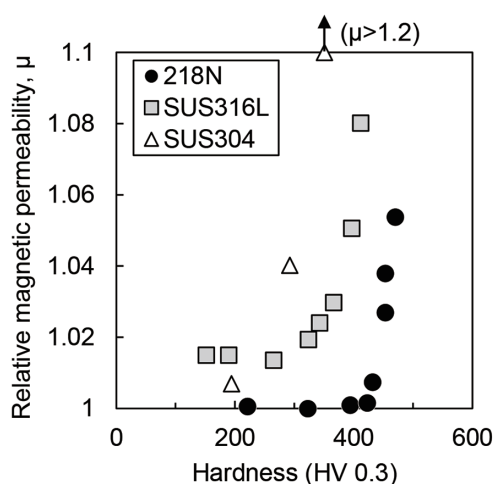


Fig. 10 Relationship of hardness and relative magnetic permeability after cold rolling

Figure 10 shows the relationship between hardness and relative permeability after cold rolling. When the hardness of SUS304 was 351 HV, its relative permeability increased to a value exceeding 1.2. This increase is presumably due to the formation of strain-induced martensite (α'). SUS316L had a low relative magnetic permeability at a hardness of up to about 300 HV, but its relative magnetic permeability was observed to increase when the hardness exceeded 300 HV. On the other hand, 218N had a low relative magnetic permeability at a hardness of up to about 400 HV, indicating an excellent balance between high strength and low magnetism. In addition to the fact that the increase in relative magnetic permeability with rolling is suppressed for steels with lower Md_{30} , 218N is essentially harder than other steels even if α' is not formed by the nitrogen addition. As a result, 218N has the potential to achieve both high strength and low magnetism simultaneously.

6. Conclusions

We investigated the optimal composition of a low-Ni, Mo-saving austenitic stainless steel for PEFC bipolar plates with crevice corrosion resistance and formability equivalent to those of SUS316L and developed 218N (21Cr-8.3Ni-0.15N). The results obtained are as follows:

- (1) In a crevice corrosion resistance test in a simulated PEFC environment, 218N was found to have crevice corrosion resistance equivalent to or higher than that of SUS316L when the [Cr+2Mo] content was 21 or higher.
- (2) In an N range of 0.10 to 0.19%, the formability (total extension) increased as the Md_{30} value increased. Also, the total extension tended to decrease as the N content increased. It was considered necessary to limit the N content to 0.19% or less to obtain a total extension of 45% or more stably.
- (3) The corrosion rate at 0.9 V, simulating the PEFC environment, decreased as the Cr content increased. According to the results of a potentiostatic test simulating a PEFC environment containing F^- ions, 218N exhibited a lower metal elution amount and a better metal elution resistance than SUS304 and SUS316L.
- (4) 218N has higher strength than SUS304 and SUS316L and exhibits particularly excellent pitting corrosion resistance and atmospheric corrosion resistance at near-room temperatures. Furthermore, it can achieve both high strength and low magnetism simultaneously. 218N is expected to find use in other applications by taking advantage of its excellent properties.

References

- 1) Nishikata, A.: Zairyo-to-Kankyo. 58, 288 (2009)
- 2) Imamura, J. et al.: Nippon Steel & Sumitomo Metal Technical Report. (106), 108 (2014)
- 3) Miyano, S. et al.: TANSO. (247), 54 (2011)
- 4) Miyazawa, A. et al.: Electrochemistry. 78 (10), 825 (2010)
- 5) NEDO: NEDO Hydrogen and Fuel Cell Achievement Report Meeting 2023, C1-16 (2023)
- 6) Yashiro, H. et al.: Zairyo-to-Kankyo. 60, 432 (2011)
- 7) Nohara, K., Ono, H., Ohashi, N.: Tetsu-to-Hagané. 63, 772 (1977)
- 8) Pourbaix, M.: Atlas of Electrochemical Equilibria in Aqueous Solutions. NACE, 1966, p.263
- 9) Pourbaix, M.: Atlas of Electrochemical Equilibria in Aqueous Solutions. NACE, 1966, p.275
- 10) Fukaya, F. et al.: Zairyo-to-Kankyo. 56, 406 (2007)
- 11) Pourbaix, M.: Atlas of Electrochemical Equilibria in Aqueous Solutions. NACE, 1966, p.498
- 12) Osozawa, K.: NETSUSHORI. (J. Jpn. Soc. Heat Treat.). 36, 206 (1997)
- 13) Yashiro, H. et al.: Zairyo-to-Kankyo. 47, 591 (1998)
- 14) Ishio, K. et al.: Tetsu-to-Hagané. 92, 38 (2006)
- 15) Tachibana, K. et al.: Zairyo-to-Kankyo. 42, 762 (1993)
- 16) Haruna, T. et al.: Zairyo-to-Kankyo. 43, 331 (1994)
- 17) Nagano, H. et al.: Materia Japan. 34, 1077 (1995)



Kotaro SEKIMUKAI
Researcher
New Energy Material Research & Development Div.
Research & Development Center
Nippon Steel Stainless Steel Corporation
3434 Ooaza-shimata, Hikari City, Yamaguchi Pref.
743-8550



Toru MATSUHASHI
General Manager, Head of Div.
Products Development Div.
Research & Development Center
Nippon Steel Stainless Steel Corporation



Kazunari IMAKAWA
Senior Researcher
Materials Reliability Research Lab.
Steel Research Laboratories



Manabu OKU
General Manager, Head of Div.
New Energy Material Research & Development Div.
Research & Development Center
Nippon Steel Stainless Steel Corporation